ISABE-2013-1215

ASSESSMENT OF THE PERFORMANCE POTENTIAL FOR A TWO-PASS CROSS FLOW INTERCOOLER FOR AERO ENGINE APPLICATIONS

Xin Zhao
Ph.D. student
Chalmers University of Technology
SE-412 96 Göteborg, Sweden
xin.zhao@chalmers.se

Tomas Grönstedt
Professor
Chalmers University of Technology
SE-412 96 Göteborg, Sweden
tomas.gronstedt@chalmers.se

Konstantinos G. Kyprianidis
Rolls-Royce Defence Aerospace
Bristol, United Kingdom
konstantinos.kyprianidis@rolls-royce.com

Abstract

The performance potential for a two-pass cross flow intercooler has been estimated through an analysis of a long range mission for a geared turbofan engine. The application of a set of CFD based correlations allows the simultaneous coupled optimization of the intercooler conceptual design parameters and the engine design. The coolant air for the intercooler is ejected through a separate variable exhaust nozzle which is used to optimize the engine performance in cruise. By comparing the optimized intercooled geared engine with an optimized advanced non-intercooled geared engine, a reduction of 4.8% fuel burn is observed.

Nomenclature

a	Major axis length of the elliptical tube
b	Minor axis length of the elliptical tube
D	Diameter
D_h	Hydraulic diameter of any internal passage
f	Friction factor
h	Heat transfer coefficient
j	Colburn j factor
K	Loss coefficient for ducts
k_{loss}	Tube internal loss coefficient
$\dot{m}$	Mass flow rate
p	Static pressure
P	Total pressure
T	Temperature
ρ	Density
ε	Roughness of the tube wall
μ	Dynamic viscosity
η	Polytropic efficiency
k	Thermal conductivity of air
Re	Reynolds number
Pr	Prantdl number
Nu	Nusselt number
St	Stanton number
BPR	Bypass ratio
FPR	Fan pressure ratio
HPC	High pressure compressor
IPC	Intermediate pressure Compressor
LPT	Low pressure turbine
OPR	Overall pressure ratio
PR	Pressure ratio
SFC	Specific fuel consumption
SFN	Specific thrust
TOC	Top of climb
NEWAC	New Aero Engine Core Concepts
LEMCOTEC	Low Emissions Core-Engine Technologies

Introduction

Intercoolers have recently received a considerable attention as a means to improve aero engine efficiency, in particular within the European research projects NEWAC and LEMCOTEC [1-8], and within the US N+3 project [9]. Intercoolers have the potential to improve engine SFC, ease the design of an efficient turbine cooling system by reducing compressor exit temperatures and hence cooling air temperatures, as well as reducing NO_x emissions. Intercooling may also provide benefits by increasing the specific output of the engine core and therefore reduce total engine weight.

Although the design of compact heat exchangers is a mature field and a wealth of design data exists [10], the availability of data directly applicable to aero engine performance studies is quite limited. Aero engine performance is strongly influenced by the weight and volume of the intercooler and the pressure losses incurred from its integration as well as the design strategy employed. Here the term design strategy refers to the sizing of the intercooler related to the mission. Within this work it is argued that it is beneficial to provide a relatively large amount of intercooling at take-off to allow for a compact engine design with a high OPR and a reduced cooling flow need. In cruise on the other hand, it is beneficial to reduce the intercooling by use of a variable intercooler exhaust nozzle, indicated in the lower part of Figure 1, to establish an optimum between intercooling and incurred pressure losses.

Another design issue that has to be addressed is to decide where in the compression process the intercooling should be introduced. An early introduction is favourable from a thermodynamic perspective whereas a later introduction will reduce the intercooler pressure losses, weight and simplify its integration by reducing the intercooler volume requirement.

Finally, the choice of the intercooler configuration itself has a decisive impact on the performance that can be achieved by an intercooled engine. It is argued here that there is a need for performance estimates that realistically represent intercoolers designed and optimized for aero engine applications.

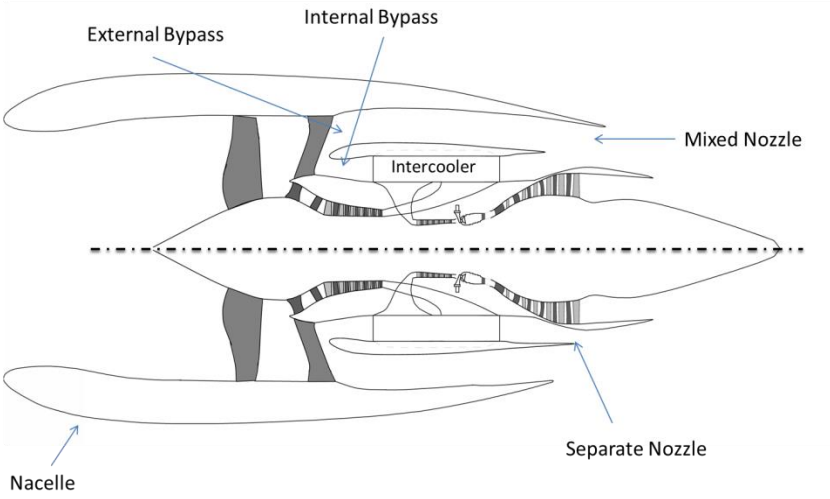

Figure 1 Intercooled engine impression [11]

This will enable engine performance in a more realistic way than can be achieved by assuming pressure loss levels or by applying simplified correlations.

The general configuration of the two-pass cross flow intercooler can be seen in Figure 2 below. Flow exiting an intermediate compressor or high speed booster enters the inflow duct through which it is diffused. The flow then enters the first stack of a tubular heat exchanger located downstream in the cooling flow direction, returns to an upstream tubular heat exchanger and then continues to an accelerating duct leading to the high pressure compressor entrance. Bypass air flows over the external surfaces of the two tubular stacks to achieve the sought intercooling. This paper extends the previous work on this concept [4, 11] by considering an involute spiral configuration for the intercooler tubes.

CFD studies for the re-designed concept was used to obtain a set of correlations which were used to evaluate the performance of a high bypass ratio intercooled geared turbofan.

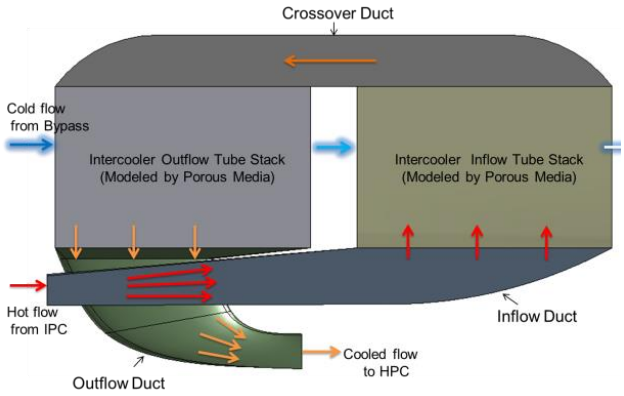

Figure 2 Two-pass cross flow intercooler impression

For a geared turbofan the LPT has a higher rotational speed than in the conventional turbofan, for which the rotational speed of the low pressure shaft is limited by the fan tip speed. For the LPT, an increased rotational speed gives a lower blade loading, higher efficiency and allows the use of fewer stages. Hence, the bypass ratio can be ultra-high without an excessive number of LPT stages. The increased shaft speed also allows for a smaller shaft diameter that makes it possible to integrate the high pressure compressor at a lower radius. This increases last stage blade height which is particularly critical for intercooled engines, which are expected to gain some of their benefits from a substantially increased OPR.

Intercooler Modelling

The correlations of the two-pass cross flow intercooler are divided into a correlation for the internal hot side connecting ducts and tubes, as well as characteristics for the external cold side staggered tubes. The general staggered tube configuration, that is the cross-section of the tube stack, can be seen from Figure 3 and the general parameters for this tube arrangement are defined in Table *1*.

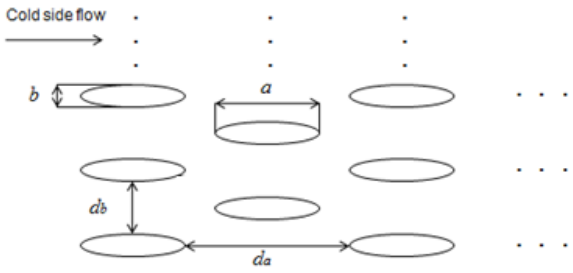

Figure 3 Intercooler external side configuration

a/b	8
d_a	a
d_b	2 b

Table 1 Tubes arrangement parameters

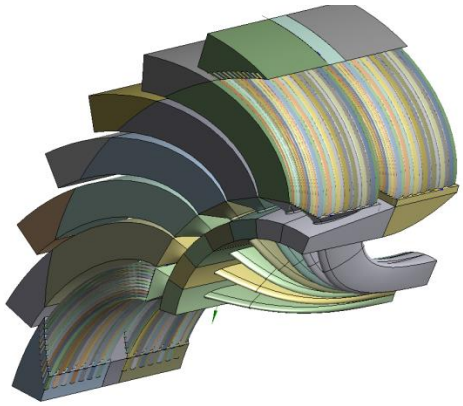

Figure 4 Involute spiral tubes configuration

An involute spiral tube configuration design is adopted for the tube stack. As seen from Figure 4 this concept gives a good utilization of the space available.

Correlations

Internal Core Side

Inflow duct (Reynolds number is based on the inflow duct inlet condition. Correlation is valid in the range of 500,000 to 1,400,000. The largest deviation from CFD data in this correlation is 0.81%):

$$K_{inflow\_duct} = -1.626 \times 10^{9} Re^{-1.837} + 0.5513$$

$$K_{inflow\_duct} = \frac{p_{out} - p_{in}}{P_{in} - p_{in}}$$

Tubes (Pressure loss correlation from [12]. Heat transfer correlation from [13]):

$$\frac{1}{\sqrt{k_{loss}}} = -1.8\log_{10}\left(\frac{6.9}{Re} + \left(\frac{\varepsilon}{D_h}/3.7\right)^{1.11}\right)$$

$$Nu = \frac{(k_{loss}/8.0)(Re - 1000)Pr}{1 + 12.7\sqrt{\left(\frac{k_{loss}}{8.0}\right)}\left(Pr^{\frac{2}{3}} - 1\right)}$$

Crossover duct (Reynolds number is based on the crossover duct inlet condition. Correlation is valid in the range of 100,000 to 350,000. The largest deviation from CFD data in this correlation is 0.78%):

$$K_{crossover\_duct} = 3.128 \times 10^{-7} Re + 10.1$$

$$K_{crossover\_duct} = \frac{p_{in} - p_{out}}{P_{in} - p_{in}}$$

Outflow duct (Reynolds number is based on the outflow duct outlet condition. The correlation is valid in the range of 1,500,000 to 5,500,000. The largest deviation from CFD data in this correlation is 0.72%):

$$K_{outflow\_duct} = 1.939 \times 10^{11} Re^{-2.1} + 0.08107$$

$$K_{outflow\_duct} = \frac{P_{out} - P_{in}}{P_{out} - p_{out}}$$

In the correlations above, p is the static pressure and P is the total pressure, while 'in' and 'out' subscripts represent the inlet and outlet of the duct respectively; ε is the roughness of the tube wall, (a value of 0.002 mm is assumed here). The hydraulic diameter of the ducts and the tube are used to calculate the Reynolds number in the corresponding correlations.

External Cold Side

The Colburn j factor is used here which is the dimensionless heat transfer coefficient as defined in [10]:

$$j = St \cdot Pr^{2/3} = \frac{Nu}{Re \cdot Pr} Pr^{2/3}$$

The Nusselt number, the Reynolds number and the related hydraulic diameter used in the external cold side correlations are calculated as:

$$D_h = \frac{4A_c L}{A_w}$$

$$Nu = \frac{hD_h}{k}$$

$$Re = \frac{(\dot{m}/A_c)D_h}{\mu}$$

where h is the local heat transfer coefficient; D_h is the hydraulic diameter of the flow passage; k is the thermal conductivity of air; A_w is the surface area of the ellipses; A_c is the minimum flow cross sectional area; L is the total flow length of the intercooler; $\dot{m}$ is the mass flow at the inlet and μ is the dynamic viscosity.

The friction factor f is defined through [10]:

$$\Delta p = \frac{(\dot{m}/A_c)^2}{2\rho_i}\left[f\frac{A_W}{A_c}\frac{\rho_i}{\rho_m} + (1+\sigma^2)\left(\frac{\rho_i}{\rho_o} - 1\right)\right]$$

where Δp is the pressure drop through the intercooler, ρ_i and ρ_o are the fluid inlet and outlet density, ρ_m is the average of ρ_i and ρ_o, σ is the ratio between the minimum flow cross sectional area A_c and the intercooler frontal area A_f.

The correlations provided below are valid in the range of 10,000 < Re < 110,000. The largest deviation from CFD data is 0.90%.

$$j = 0.003469e^{-7.117\times10^{-5}Re} + 0.003461e^{-3.793\times10^{-6}Re}$$

$$f = 0.01044e^{-6.806\times10^{-5}Re} + 0.008109e^{-2.908\times10^{-6}Re}$$

Furthermore, the additional weight and nacelle diameter caused by the intercooler has been considered. Titanium is assumed to be used as intercooler material. The tube thickness is calculated based on the pressure difference between the inner and outer side of the tube. A minimum tube thickness is assumed to be 0.2 mm. The nacelle line moves with the change in intercooler size, in order to keep the external bypass flow Mach number lower than 0.6.

Engine modelling

The advanced non-intercooled geared engine is optimized by varying the bypass ratio, fan, IPC and HPC pressure ratio. The OPR is limited due to the turbine blade and disc cooling temperature, as manifested by a maximum compressor exit temperature of 950 K. The engine take-off net thrust is set to be 65625 lbf which is considered suitable for the twin engine aircraft model used for this study. Design point data and constraints common to the geared and the intercooled geared engine are summarized in Table 2 below. The efficiencies in the table are polytropic. T_{blade} is the allowed maximum blade temperature. A hot day take-off condition is used to evaluate the engine at the start of the mission analysis. The cooling flow is then calculated based on the model established in [14].

Parameter	Value
$T_{HPC,exit}$	< 950 K
$T_{Combustor,exit}$	< 1900 K
T_{blade}	< 1210 K
η_{fan}	93.5%
η_{IPC}	92.2%
η_{HPC}	92.5%
η_{HPT}	90.7%
η_{IPT}	91.4%
η_{LPT}	93.25%
Net Thrust	65625 lbf

Table 2 Design point performance parameters (take-off)

The data presented in Table 2 are based on estimates on performance levels achievable for an engine entering into service year 2020+. The optimization procedure establishes an engine that provides minimum fuel burn for a fixed

mission and fixed aircraft. The mission length is 6800 km. Initial cruise altitude is 35000 ft and final cruise altitude is 39000 ft. A trade factor is established to estimate the full fuel burn saving potential for a scalable aircraft.

With the optimization of the intercooler parameters, the mission study has more design freedom and is more complicated than analysing the advanced non-intercooled engine. The basic intercooler parameters to be determined are the tube diameter, the tube length, the number of rows and number of columns.

The intercooler coolant mass flow is being controlled by a separate variable geometry exhaust nozzle. The exhaust nozzle area is hence included as part of the optimization parameters. Closing the nozzle reduces intercooler external Mach numbers and related pressure losses, both over the intercooler tubes and in the upstream intercooler diffuser. The closing of the nozzle also decreases transferred heat, which leads to an increased combustor inlet temperature and a reduced fuel flow need. The increased compressor power requirement results in an increased turbine inlet temperature and also a somewhat increased temperature in the core exhaust nozzle. In total this process reduces the thermal efficiency but this is outweighed by the strong reduction in irreversibilities generated in the intercooler.

The tube diameter is controlled by the major axis length of the tube, since the aspect ratio is fixed. As the size of the tube is decreasing, the total perimeter length of the tubes increases for a given cross sectional area which leads to an increase of the wetted area.

The tube length, which is set by the radial position of the diffuser and the inner diameter of the internal bypass duct, has the limitation of keeping the external bypass flow Mach number, the nacelle maximum diameter and the internal bypass diffusion loss down. However, an increased tube length gives larger frontal area which in turn gives a lower flow Mach number through the intercooler and hence a lower intercooler external side pressure loss.

Basically, the total heat transfer area is determined by the single tube size and the number of tubes. The number of tubes is equal to the number of tube rows (circumferential direction) multiplied by the number of tube columns (axial direction). The distribution between the number of rows and the number of columns plays an important role in the intercooler performance. Generally, with a given single tube size and heat transfer area, fewer columns are desirable for decreasing the external side pressure loss. A high radius installation of the intercooler gives more rows and fewer columns but also increases the nacelle diameter.

The design parameters determining the basic intercooler parameters are given in Table 3. Here, a is the major axis length of the inside of the elliptical tube, D_i is the hub diameter of the intercooler matrix, D_o is the diameter of the shroud of the intercooler and M_{tube} is the flow Mach number inside the tubes. M_{tube} and a are input to the design process whereas D_i and D_o are obtained from the conceptual design of the engine.

The conceptual design process used here, apart from the intercooler design has been outlined in [11] and is described in more detail in [15, 16]. The weight calculation is integrated in the optimization process and changes for every new

engine/aircraft mission being evaluated.

Basic intercooler parameters	**Design parameters**		
Tube diameter	a		
Tube length	D_i	D_o	
Number of Tube rows	D_i	a	M_{tube}
Number of Tube columns	D_i	a	M_{tube}

Table 3 Intercooler design parameters

Results and Discussions

For the advanced non-intercooled geared turbofan engine, the optimal OPR (take-off) is found to be 61, whereas for the intercooled engine an OPR of 81 is obtained. For the intercooled geared turbofan, a further reduction in mission fuel burn can be achieved for an even higher OPR. However, the minimum compressor blade height constraint of the HPC then becomes active. A rule of thumb is that the compressor blade height should not be lower than 12 mm and the hub tip ratio should be kept lower than 0.92, otherwise, the tip clearance loss and end wall boundary layer losses of the HPC will deteriorate its efficiency.

In order to reduce the number of design parameters, the flow Mach number inside the tubes (M_{tube}) is fixed to be 0.07. This was done after a number of preliminary optimization studies revealed that the optimizer always produced the lowest internal tube Mach number possible. Lower values lead to designs that could not be fitted within the available space constraints. Attempts to increase the external nacelle diameter to accommodate a larger intercooler resulted in an increase in mission fuel burn.

A cruise SFC benefit of 3.2% is observed for the intercooled engine, as seen in Table 4. For the fixed aircraft mission this integrated to a 3.2% fuel burn benefit. The SFC reduction is due to a higher thermal efficiency resulting from a higher OPR and a reduced cooling flow need.

	Advanced non-IC	Intercooled
OPR	61	81
TOC OPR	76	101
Cruise OPR	58	75
BPR	15.42	16.74
Fan PR	1.40	1.44
IPC PR	4.91	4.55
HPC PR	7.72	13.78
HPC last blade height (mm)	19.4	13.6
Take-off HPC exit temperature (K)	941.9	888.4
HPT Cooling bleed ratio	0.19	0.14
Take-off SFC (mg/Ns)	6.28	6.17
TOC SFC (mg/Ns)	13.07	12.93
Cruise SFC (mg/Ns)	13.10	12.68
Cruise $\eta_{thermal}$	0.514	0.524
Cruise $\eta_{propulsive}$	0.823	0.810
a (mm)	NA	30.7
Tube Length (m)	NA	0.37
Rows	NA	11
Columns	NA	20
Intercooler Weight (kg)	NA	309
Engine Weight (kg)	7005	6705
Nacelle Diameter(m)	3.47	3.41
Mission fuel burn (kg)	30425 Base	29440 -3.2%

Table 4 Optimal engine configurations

In addition, the intercooler also contributes to a reduced engine core size through an increase in the specific power of the core,

resulting in an estimated 300 kg weight reduction. The nacelle diameter is only slightly reduced for the intercooled engine contributing only marginally to the reduced fuel burn.

A trade factor was established to take into account that the reduced fuel burn can be used to reduce the aircraft operational empty weight and take-off weight. The trade factor also takes into account that the reduced take-off weight allows for a reduced aircraft drag and a reduced engine thrust. The value of the trade factor was estimated at 1.5 which gives a net fuel burn reduction of 4.8%.

	Take-off	Top of Climb	Mid Cruise
OPR	81	101	75
Core Flow Temperature Drop (K)	87	72	59
Core Pressure loss	3.7%	5.0%	4.6%
Coolant flow Pressure loss	14.5%	10.9%	4.0%
Coolant mass flow (kg/s)	111	38	16
Altitude(ft)	0	35000	39000
Mach number	0	0.81	0.81
Net Thrust (lbf)	66040	15191	8351
$\eta_{thermal}$	0.449	0.531	0.524
$\eta_{propulsive}$	0	0.757	0.810

Table 5 Intercooler operation conditions (Optimal engine configuration)

From Table 5 above it can be seen that the take-off point demands the highest amount of intercooling. For the top-of-climb and cruise points, the heat transfer can be reduced by controlling the separate nozzle to reduce the coolant mass flow. With a lower coolant mass flow, less heat rejection from the core to the external bypass leads to a higher thermal efficiency and propulsive efficiency. Additionally, the flow over the external intercooler surface, which is associated with a relatively high pressure loss, is reduced. This will also add to the improvement of the thermal efficiency.

The minimum mission fuel burn for the intercooled engine is remarkably insensitive to BPR variation as is indicated by Table 6 below. From comparing the cruise point SFC and engine size, the 14.5 BPR engine benefits from lower nacelle drag and engine weight while the higher BPR engine has a greater SFC benefit.

OPR	81	81	81
BPR	14.50	15.50	16.74
Fan PR	1.50	1.48	1.44
IPC PR	4.70	4.59	4.55
a (mm)	29.4	29.0	30.7
Number of tube columns	22	21	20
Tube Length (m)	0.38	0.39	0.37
Nacelle Diameter(m)	3.30	3.34	3.41
Engine Weight (kg)	6385	6438	6705
Cruise SFC (mg/Ns)	12.88	12.78	12.68
$\eta_{thermal}$	0.524	0.525	0.524
$\eta_{propulsive}$	0.797	0.802	0.810
Mission Fuel burn	29555	29449	29440

Table 6 Intercooled configurations for a parametric BPR variation (the last column is the optimal engine)

From BPR 15.5 to 16.74, there is a LPT stage increase due to that the stage loading in the LPT has reached its limit. An additional LPT stage gives a step increase in weight and hence a step increase in fuel burn. However, the reduced FPR implies reduced specific thrust and hence an improved propulsive efficiency. Additionally, as the BPR is increasing, the fan size increases as well as the nacelle

line. This actually gives more space for the intercooler installation and then the intercooler is installed in a higher radial position. As mentioned before, a higher radial position gives fewer columns which are desired for reducing the intercooler pressure losses. The tube length has been reduced as well due to the increased radial position of the intercooler installation. This leads to a reduction in the internal side pressure loss.

The combined effect offsets the weight penalty from the additional LPT stage. The optimal engine is then defined at BPR 16.74. A further increase in BPR will result in an increase in fuel burn due to that the nacelle drag starts to dominate.

Conclusions

In general the two-pass cross flow intercooler has been seen to give a relatively small internal pressure loss. A relatively high external pressure loss has been observed, but this could be limited quite effectively in cruise by the use of the variable exhaust nozzle. The transferred heat with this intercooler concept is relatively modest. It is however sufficient to enable the higher OPR which is restricted by the compressor exit temperatures for the advanced non-intercooled geared engine. An OPR of 75 was achieved in cruise compared to an OPR of 55 for the advanced non-intercooled engine. The intercooled engine OPR is actually higher if the auxiliary nozzle area is kept at its design value, but there is a net gain in fuel burn reduction from reducing its area. The intercooling also allowed for a somewhat smaller engine giving a marginal benefit in nacelle drag reduction and a somewhat larger effect due to a reduced weight. A larger benefit is obtained from the reduced compressor exit temperature which gives a reduced cooling flow need. Potentially the reduced compressor exit temperature could also be used to reduce NO_x emissions.

Acknowledgement

This work is financially supported by the E.U. under the "LEMCOTEC – Low Emissions Core-Engine Technologies", a Collaborative Project co-funded by the European Commission within the Seventh Framework Programme (2007-2013) under the Grant Agreement n° 283216.

We also would like to thank Richard Avellán and Anders Lundbladh at GKN Aerospace, and Andrew Rolt at Rolls-Royce for valuable discussions.

References

[1] Kyprianidis, K., Rolt, A. M., and Grönstedt, T., '*Multi-Disciplinary Analysis of A Geared Fan Intercooled Core Aero-Engine*'. Proceedings of ASME Turbo Expo 2013, San Antonio, Texas, USA, GT2013-95474, June 2013.

[2] Xu, L., Kyprianidis, K., and Grönstedt, T., '*Optimization Study of an Intercooled Recuperated Aero-Engine*'. AIAA Journal of Propulsion and Power, Vol. 29, No.2, pp.424-432, 2013.

[3] Kyprianidis, K., Grönstedt, T., Ogaji, S., Pilidis, P., and Singh, R., 'Assessment of Future Aero-Engine Designs with Intercooled and Intercooled Recuperated Cores', ASME Journal of Engineering for Gas Turbines and Power, 133(1), doi:10.1115/1.4001982 January 2011.

[4] Xu, L. and Grönstedt, T., '*Design and Analysis of an Intercooled Turbofan Engine*'. ASME Journal of Engineering for Gas Turbines and Power, Vol. 132, No. 11, doi:10.1115/1.4000857 Nov 2010.

[5] Grönstedt, T. and Kyprianidis, K., '*Optimizing the Operation of the Intercooled Turbofan Engine*'. Proceedings of ASME Turbo Expo 2010: Power for Land, Sea and Air, Glasgow, UK, ASME GT2010-22519, June 2010.

[6] Rolt, A. M. and Baker, N. J., '*Intercooled Turbofan Engine Design and Technology Research in the EU Framework 6 NEWAC Programme*'. The 19th International Symposium on Air Breathing Engines, Montreal, Canada, ISABE-2009-1278, 2009.

[7] Rolt, A. M. and Kyprianidis, K., '*Assessment of New Aeroengine Core Concepts and Technologies in The EU Framework 6 NEWAC Programme*'. 27th International Congress of The Aeronautical Sciences, Nice, France, ICAS 2010-4.6.3, Sep 2010.

[8] Lundbladh, A. and Sjunnesson, A., '*Heat Exchanger Weight and Efficiency Impact on Jet Engine Transport Applications*'. 16th International Symposium on Air Breathing Engines, Cleveland, Ohio, ISABE-2003-1122, Sep 2003.

[9] Bruner, S., Baber, S., Harris, C., Caldwell, N.,Keding, P., Rahrig, K., Pho, Luck., and Wlezian, N., '*NASA N+3 Subsonic Fixed Wing Silent Efficient Low-Emissions Commercial Transport (SELECT) Vehicle Study*', NASA/CR-2010-216798, Nov, 2010.

[10] Kays, W. M., and London, A. L., *Compact Heat Exchanger*, 2nd ed. McGraw-Hill, ISBN 07-033391-2. 1964.

[11] Xu, L., '*Analysis and Evaluation of Innovatiove Aero Engine Core Concepts*', Ph.D Thesis, Chalmers University of Technology, Sweden, 2011.

[12]Haaland, S. E., '*Simple and Explicit Formulas For the Friction Factor in Turbulent Pipe Flow*'. J.Fluids Eng., 105(1), pp. 89-90. 1983.

[13] Gnielinski, V., '*New Equations for Heat and Mass Transfer in Turbulent Pipe and Channel Flow*'. International Chemical Engineering, 16, pp. 359-368. 1976.

[14] Wilcock, R.C., Young, J.B., and Horlock, J.H., '*The Effect of Turbine Blade Cooling on the Cycle Efficiency of Gas Turbine Power Cycles*'. Journal of Engineering for Gas Turbines and Power, 127, Jan, pp. 109-120, 2005

[15] Grönstedt, T., Au, D., Kyprianidis, K. and Ogaji S., '*Low-Pressure System Component Advancements and Its Influence on Future Turbofan Engine Emissions*', GT2009-60201, ASME Turbo Expo 2009, Florida, Orlando, USA, 2009.

[16] Kyprianidis, K., Au, D., Ogaji, S. and Grönstedt, T., '*Low Pressure System Component Advancements and its Impact on Future Turbofan Engine Emissions*', ISABE-2009-1276, Montreal, Canada, 2009.